UDK621.3:(53+54+621+66), ISSN0352-9045 Informacije MIDEM 34(2004)3, Ljubljana

SILICON-GLASS ANODIC BONDING

Uroš Aljančič, D. Resnik, D. Vrtačnik, M. Možek, S. Amon

University of Ljubljana, Faculty of Electrical Engineering, Laboratory of Microsensor Structures and Electronics - LMSE, Ljubljana, Slovenia

Key words: anodic bonding, silicon, Pyrex glass, piezoresistive pressure sensor

Abstract: Piezoresistive pressure sensors test structures fabricated on the same silicon wafer were anodic bonded to Pyrex glass wafer and bonding characteristics were analyzed. Surface profiles of both, silicon and Pyrex wafer, were measured before and after bonding process using Taylor-Hobson Talysurf surface profiler. A simple test method for non-destructive in-situ evaluation of both, anodic bonding parameters and bond quality was introduced. Possible causes for thin silicon diaphragms deflection, detected after anodic bonding process, were analyzed and discussed.

Anodno bondiranje silicij - steklo

Kjučne besede: anodno bondiranje, silicij, Pyrex steklo, piezorezistivni senzor tlaka

Izvleček: Testne strukture piezorezistivnega senzorja tlaka so bile anodno zbondirane na rezino Pyrex stekla. Površinski profili obeh rezin pred in po bondiranju so bili posneti s Taylor-Hobson-ovim površinskim profilometrom. Vpeljana je preprosta metoda za nedestruktivno oceno bondirnih parametrov in kvalitete bonda, ki je uporabna tudi med samim tehnološkim procesom. Merilni rezultati na testnih strukturah s tanko silicijevo membrano kažejo ukrivljenost membrane po zaključenem bondirnem procesu. Raziskani so bili možni vzroki za takšno obnašanje testnih struktur.

1. Introduction

Since Wallis and Pomeratz /1/ first introduced anodic or electrostatic bonding in 1969, this technique became one of the basic steps in the fabrication of micro-electro mechanical systems (MEMS). Beside usage of anodic bonding for joining silicon wafer to glass wafer, several related techniques were developed in recent years such as anodic bonding using sputtered glass /2,3/, evaporated glass /4-6/ and spin-on glass /7/. These methods are used for vacuum packaging, hermetic sealing, and encapsulation of MEMS as well as fabrication of reference cavities for pressure and acceleration sensors.

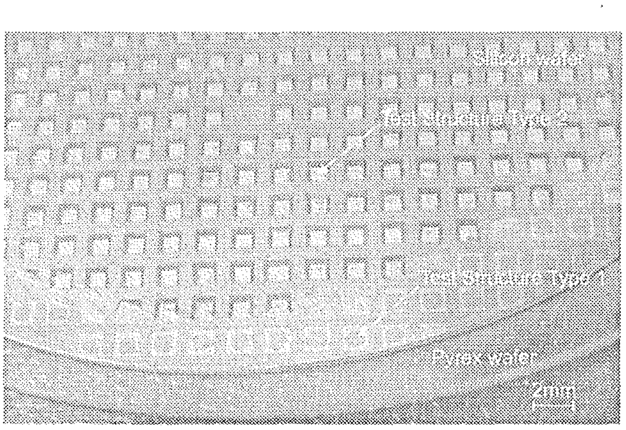

Figure 1: Pyrex wafer bonded to silicon wafer with piezoresistive pressure sensor structures (type2). Pressure sensors structures without diaphragm (type1) are located at the wafers edge

In this paper, 7740 Corning Pyrex glass wafers were anodically bonded to silicon wafers with pressure sensor structure (Fig.1). Among similar commercially available glasses, the main reason to choose 7740 Pyrex glass wafers in our case was their thermal expansion coefficient, well matched with silicon in a wide temperature range. In addition, relative low volume resistivity of 7740 Pyrex glass enables formation of reliable bond already at low applied voltage and temperature that could be essential in many applications. Despite the fact that the optimal solution is to bond silicon wafer directly to glass, silicon oxide as an intermediate layer was introduced in our case to analyze the effects during the bonding of structurized silicon wafers to flat Pyrex glass wafers.

Two different types of test piezoresistive pressure sensor structures fabricated on the same wafer were investigated. The only difference between both is that in the first structure anisotropic etching of diaphragm is not performed. These structures (type1), located in narrow area at the wafers edge (Fig.1), were used as the bond strength test structures based on the blade insertion technique /8-12/ to induce delamination. The second test structures (type2) were used to study fabrication of reference cavity under pressure sensor diaphragm.

2. Bonding mechanism

Bonding mechanism itself is not yet completely understood, but it is generally agreed that bonding is primarily due to the presence of mobile sodium ions in Pyrex glass. At elevated temperatures (yet below the softening point of Pyrex at 821 °C), positive sodium ions are mobile enough for Pyrex to behave like conductor (Fig.2).

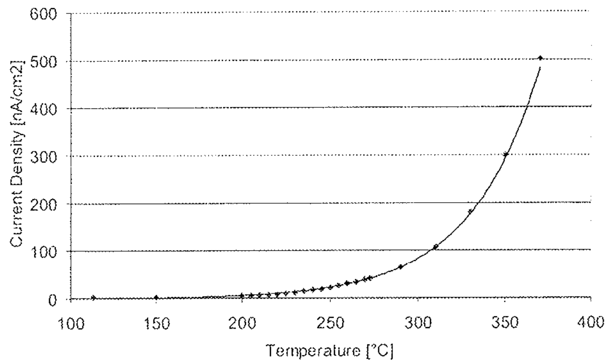

Figure 2: Steady state current density vs. temperature measured through 725μm thick 7740 Corning Pyrex glass wafer between two aluminium electrodes.

When a DC voltage (V) is applied across the silicon-glass sandwich (Fig.3a), sodium ions in glass are transported toward the cathode. The more strongly bounded negative oxygen ions in glass are left in glass adjacent to the silicon surface, forming negative space charge layer. This negative charge layer in glass, together with positive charge in silicon, creates a high electrostatic field across thin air gap between both surfaces. As a consequence, a strong electrostatic pressure pulls both wafers into intimate contact (Fig.3a). This effect can be easily observed during the bonding process on transparent Pyrex glass as the light grey interface between silicon and glass becomes dark grey.

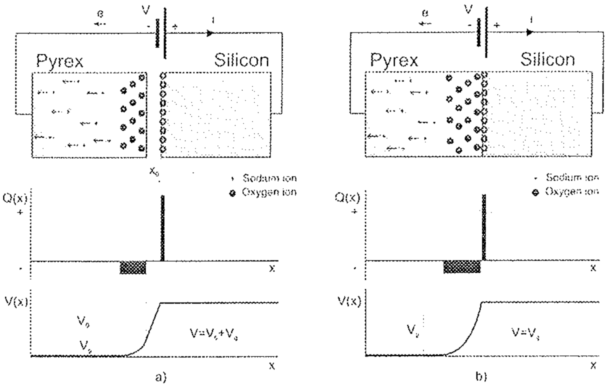

Figure 3: Charge and potential distribution during anodic bonding process: a) before and b) after intimate contact between silicon and Pyrex wafer

Once wafers are in intimate contact (Fig.3b), almost all of the applied voltage (V) is dropped across the narrow space charge layer in glass (V_g), resulting in extremely high field, strong enough to develop transport of oxygen ions to the bonding surface. As a consequence, irreversible Si-O-Si bonds in the interface, joining Pyrex and silicon, are presumed to occur.

3. Experimental

Test structures of silicon pressure sensors, fabricated on 3-inch, CZ grown, <100> crystallographic oriented, 20Ohmcm, n-type, 374μm thick, double side mechanically polished silicon wafers (details reported elsewhere /13/) were bonded to commercially available 4-inch, 725μm thick 7740 Corning Pyrex glass wafers (Figs.1,4). Before bonding, a thin layer of silicon nitride (70nm) - that covers thin silicon oxide (500nm) on the backside of test structure used for mask during diaphragm etching in KOH - was removed in RIE plasma etcher.

During etching of 20μm thick pressure sensor diaphragms, silicon wafer was placed to a holder that protects wafer front-side from aggressive KOH. Because of the holder sealing, a narrow region at the edge of silicon wafer backside was also protected from KOH etching. This is the reason why diaphragms near wafers edge are not etched (Fig.1). This un-etched region was used in our case for the non-destructive anodic bond strength characterization /15, 16, 17/.

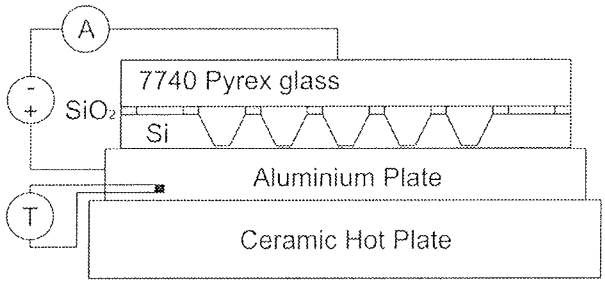

Figure 4: Anodic bonding process setup.

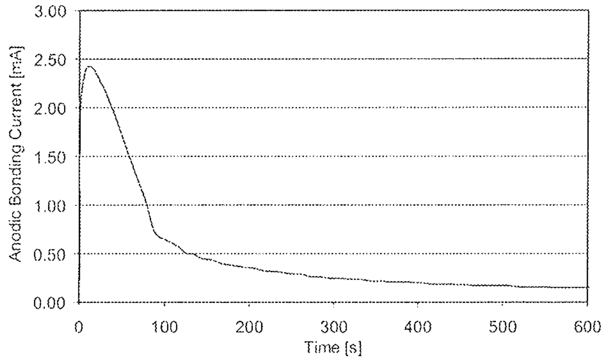

Figure 5: Typical anodic bonding current vs. time.

After surfaces of both wafers were characterized with Taylor-Hobson Talysurf surface profiler, they were cleaned with DI water and dried with nitrogen. As suggested by Resnik et al. /14/, both wafers were put into an intimate contact in cleanroom ambient at room temperature immediately after surface preparation to avoid particles that cause voids. Silicon-Pyrex structure was bonded together by applying high DC voltage (730V) at temperature 370°C in air atmosphere, using Cimarec hot plate with ceramic top (Fig.4).

Bonding temperature was monitored by thermocouple mounted in aluminium plate. Anodic bonding current was measured during bonding process and a typical result is shown in Fig.5. After bonding process, the surface was scanned again in the same areas as before, using the same Talysurf surface profiler setup.

4. Results & discussion

4.1 Structure without diaphragm (type 1)

Surface profiles (Figs. 6-11) of test structures without diaphragm from the wafer edge (Fig.1) were scanned with Talysurf in length of 1.7mm with speed of 0.5mm/s. Profiles were normalized, i.e. rotated till beginning and end of measured curve was in horizontal line.

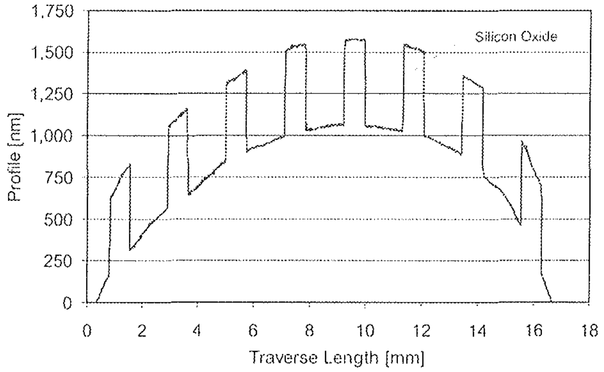

Figure 6: Surface profile of silicon wafer back-side covered with 500nm thin silicon oxide mask scanned at wafer edge before bonding. Diaphragms of pressure sensors at the wafers edge were not etched.

Before anodic bonding, silicon and Pyrex glass wafer were scanned on both sides (Figs.6-9). In Fig.6, surface profile of silicon wafer back-side is shown. Steps in this profile (Fig.6) originate in approx. 500nm thick silicon oxide square diaphragm mask (Fig.1), which is used here as anodic bonding strength test structure. Surface profile of silicon wafer front-side (before bonding) in Fig.7 also contains groups of steps, originating in approx. 500nm thick aluminium metallization lines of pressure sensor. Surface scan of Pyrex glass wafer both sides, front and back, before anodic bonding procedure are presented in Figs.8 and 9, respectively.

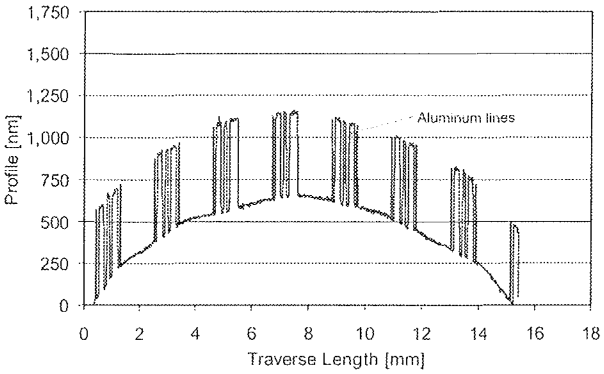

Figure 7: Surface profile of silicon wafer front-side scanned at wafer edge before bonding. Peaks represent 500nm thin aluminium metallization lines of single pressure sensor.

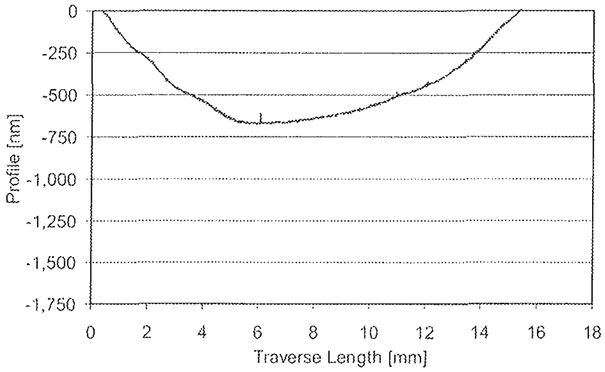

Figure 8: Surface profile of Pyrex glass wafer front-side before bonding.

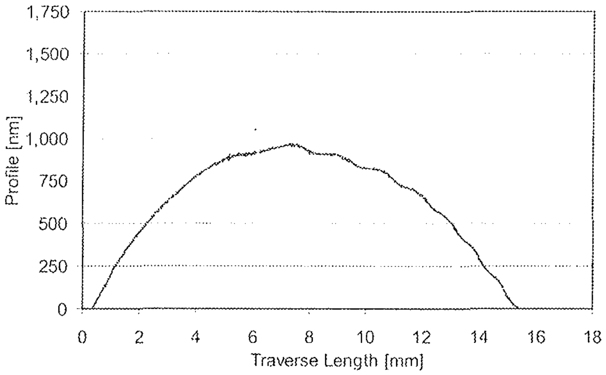

Figure 9: Surface profile of Pyrex glass wafer back-side before bonding.

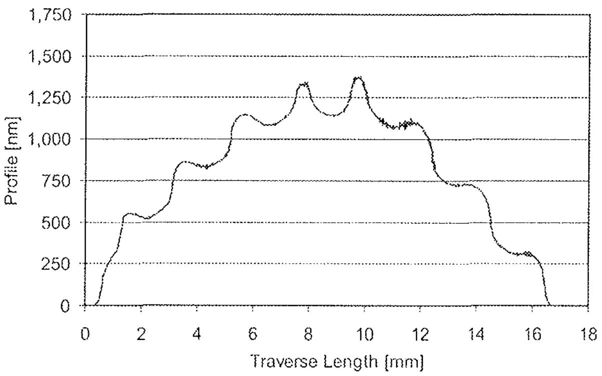

Figure 10: Surface profile of Pyrex glass wafer front-side after bonding.

After silicon and Pyrex wafers were anodically bonded together, with back-sides in contact, surface scans of bonded wafers front-sides were repeated in the same areas as before. Results are presented in Figs.10-11. In both figures, it is clearly seen again the modulated surface profiles with silicon oxide mask as before on Fig.6. Similar amplitudes of modulated surface profile were measured on both surfaces (240µm on Pyrex surface (Fig.10) and 260µm on silicon surface (Fig.11)).

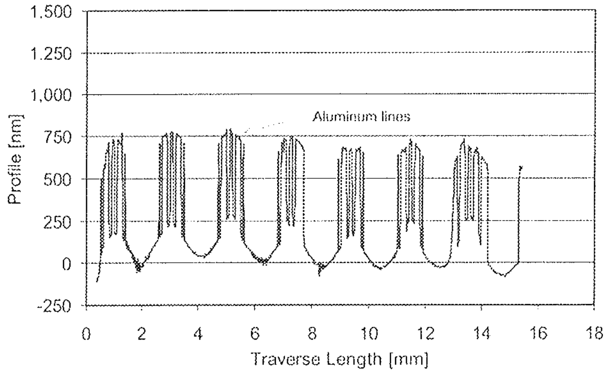

Figure 11: Surface profile of silicon wafer front-side after bonding.

Measured results clearly show that both, silicon and Pyrex wafer bend within test structure with silicon oxide mask. Bonding plane lies at 260nm from the interface between silicon and silicon oxide (Fig.12). From several measuring methods, the strength of the bond between two wafers of different material can be evaluated by technique developed on double cantilever cracking under constant wedging condition (Fig.13) /8-12/. In our case, both parameters, blade thickness (2h) and crack propagation (c) were substituted by thickness of thin silicon oxide mask (500nm) and by distance between mask and bonding point of both wafers at the centre of diaphragm (135µm in Fig.12), respectively.

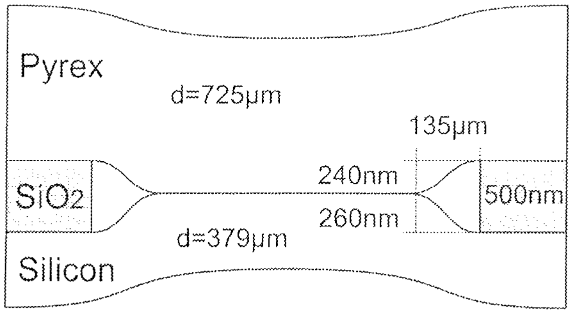

Figure 12: Cross-section of bond test structure with measured parameters

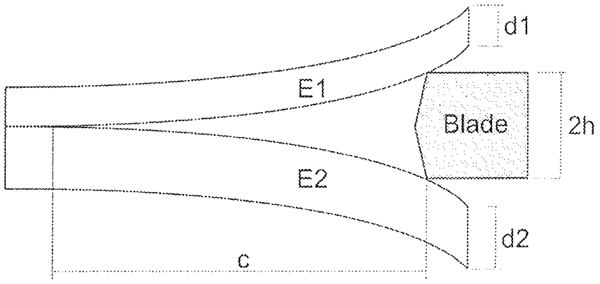

Figure 13: Double cantilever test geometry under wedging condition

In contrast to silicon-silicon wafer bonding, in silicon-Pyrex anodic bonding, the distance c between mask and bond is easily determined by optical microscope. Because bonding within test structure occurs if bond energy is greater than the value determined by blade technique, work of adhesion W_{AB} (per unit area) can be expressed as /12/:

$$W_{AB} \geq \frac{3h^2 E_{Si} d_{Si}^3 E_g d_g^3}{2c^4 (E_{Si} d_{Si}^3 + E_g d_g^3)} \approx 1.65 GPa\mu m \qquad (1)$$

where $2h$ is silicon oxide mask thickness, c is distance between mask and bond, d_{Si} is thickness of silicon wafer, d_g is thickness of Pyrex wafer, and E_{Si} and E_g are Young's -modulus of silicon and Pyrex, respectively. It is necessary to emphasize that the determined work of adhesion W_{AB} = 1,65GPaµm, represents a quantitative estimation of bond strength between silicon and Pyrex within the test structure. Therefore, the presented approach based on simple test structure can be used for in-situ non-destructive evaluation of both, anodic bonding process parameters and bond quality, as a comparative method on different parts of a single wafer, between wafers in one run and between different runs as well.

4.2 Structure with diaphragm (type 2)

Test structures with 20µm thick diaphragm were characterized in the same manner as structures without diaphragms. Surface profile scans of these structures are presented in Figs.14-17. Despite thin silicon diaphragm, no particular difference was observed in surface profile scan at the centre of silicon wafer front-side before bonding (Fig.14) compared to scan at the edge of silicon wafer shown in Fig.7. On the other hand, silicon wafer back-side profile in wafers centre before bonding (Fig.15) shows distinctive property of anisotropic etched silicon wafer. Etching depth of 354µm was measured in presented scan.

Compared to structures without diaphragms, no significant differences were obtained from surface scans of Pyrex glass either before or after bonding procedure. This is the reason why those scans are not presented here. Much more interesting results were found in surface scan of silicon wafer front-side after bonding procedure (Figs.16, 17). A magnified section of scanned profile in Fig.16 is presented in Fig.17.

After bonding procedure, deflection peaks in value of 500nm were measured on 20µm thin silicon diaphragms

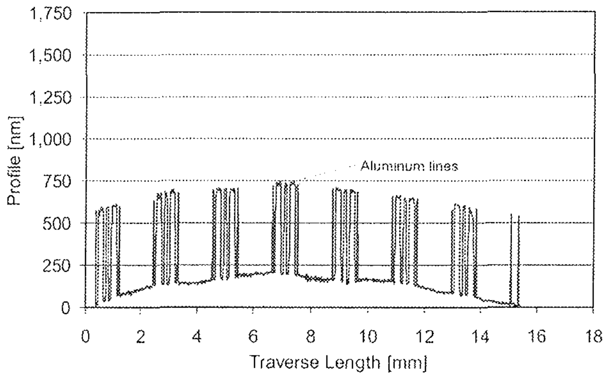

Figure 14: *Surface profile of silicon wafer front-side scanned at wafer centre before bonding. Peaks represent 500nm thin aluminium metallization lines of single pressure sensor.*

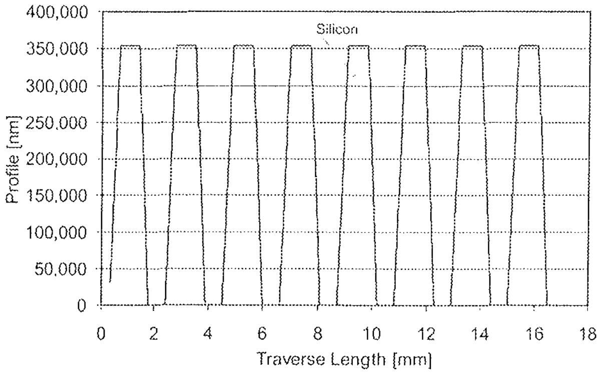

Figure 15: *Surface profile of silicon wafer back-side scanned at wafer centre before bonding. Peaks represent 354µm thick anisotropic etched silicon wafer bulk.*

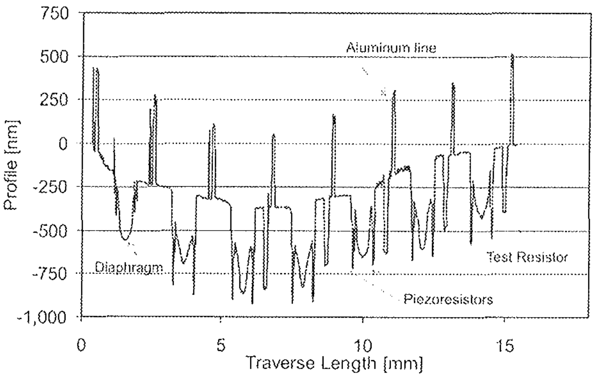

Figure 16: *Surface profile of silicon wafer front-side scanned at wafer centre after bonding shows deflection of pressure sensor diaphragm.*

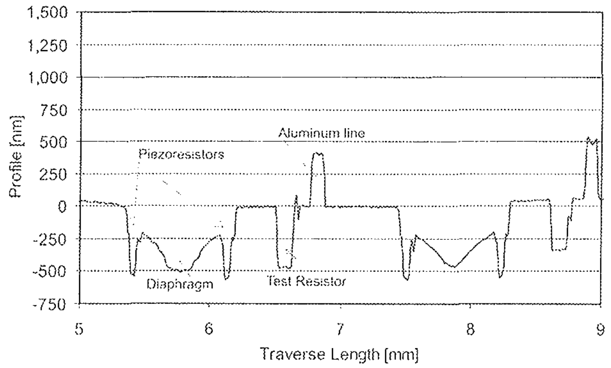

Figure 17: *Zoom of surface profile of silicon wafer front-side scanned at wafer centre after bonding shows deflection of pressure sensor diaphragm.*

(Figs.16, 17). This result was the reason for a further study of its origins. First, electrostatic pressure involved during anodic bonding procedure was investigated as the possible cause for mentioned deflection. In the first moment, when a high DC voltage is applied to the silicon-Pyrex structure, value of electrostatic pressure *p* under non-deflected diaphragm can be calculated from the following equation /18/:

$$p=\frac{1}{2}\varepsilon_0\varepsilon_r\frac{V^2}{h^2} \qquad (2)$$

where *V* represents applied DC voltage (assuming neglectable depth of space charge layer in Fig.3), *h* is the distance between silicon diaphragm and Pyrex glass, ε_0 is permittivity of free space (the ideal vacuum), and ε_r is dielectric constant or relative permittivity of air (1,00059). Due to 354µm thick air gap *h* between silicon diaphragm and Pyrex glass, a value of 18.8Pa was determined for electrostatic pressure that press diaphragm toward glass during anodic bonding procedure. This amount of electrostatic pressure can easily be neglected.

Next, thermally induced mechanical stress as possible cause for diaphragm deflection was studied. As presented elsewhere /19/, thin silicon diaphragm could deflect at elevated temperature due to the mismatch of thermal expansion coefficients of thin layers that covers the diaphragm, despite the fact that the residual mechanical stress in diaphragm at room temperature could be neglected. However, this deflection disappears when such a structure is cooled down to room temperature. This is the reason that thermally induced mechanical stresses were also rejected as the cause for measured diaphragm deflection.

Finally, due to the fact that anodic bonding procedure was done at normal air pressure (10^5Pa), the main reason for diaphragm deflections, presented in Figs.16 and 17 was found in the well known gas equation:

$$\frac{p_1V_1}{T_1}=\frac{p_2V_2}{T_2}=const. \qquad (3)$$

where p_1 represents air pressure, V_1 is reference cavity volume during anodic bonding procedure at elevated temperature T_1, while p_2 means pressure (vacuum) under thin diaphragm in reference cavity with volume V_2 at room temperature T_2. Compared to reference cavity volume V_1, change of cavity volume V_2 due to the deflected diaphragm is neglectable in our case. Because both wafers, silicon and Pyrex, came into intimate (hermetic) contact at air pressure and temperature 370°C immediately after DC voltage was applied, pressure (vacuum) in reference cavity p_2 in value of 6.49kPa was determined from Eq.3. The same diaphragm deflection can be achieved, if pressure of 93,51kPa is applied on the diaphragm from above.

Using our laboratory computer simulator for thin silicon diaphragm deflections /20/, pressure above 500nm deflected thin silicon diaphragm was determined. Simulations for piezoresistive pressure sensor structure deflection show that such a diaphragm deflects for 500nm (maximal deflection in centre of diaphragm) in case when pressure of 77.88kPa is applied to its top surface.

Simulated result (77.88kPa) does not match with the result obtained from gas equation (93.51kPa). The reason for that could be oxygen generation during anodic bonding procedure, an assumption widely accepted in the literature /21,22/.

5. Conclusion

Test structures, based on piezoresistive pressure sensors were anodic bonded to Pyrex glass and analyzed. Surface profiles of both, silicon and Pyrex wafer, were measured before and after bonding process, using Taylor-Hobson Talysurf surface profiler. A simple test method for non-destructive in-situ evaluation of both, anodic bonding parameters and bond quality, was introduced. Anodic bond strength between 7740 Corning Pyrex glass wafer and silicon wafer was determined. Measured results on test structure without diaphragm unambiguously show bending of both, silicon and Pyrex wafer. Bond strength within test structures was evaluated by a new technique developed on double cantilever cracking under constant wedging condition. The proposed approach is appropriate for a simple, efficient quality control in anodic bonding process. Measured results on test structures with thin silicon diaphragm show diaphragms deflection after the anodic bonding process was performed. Possible causes for such behaviour were analyzed and discussed.

Acknowledgements

This work was supported by Ministry of Science, Education and Sport of Republic of Slovenia.

6. References

/1/ G.D.Wallis, D.I. Pomeratz, Field assisted glass-metal sealing, J.Appl.Phys. 40, 1969, 3946-3948

/2/ A.Hanneborg et al., Silicon to thin film anodic bonding, J. Micromech. Microeng. 2 1992, 117-121

/3/ J. Berenschot et al., New applications of r.f.-sputtered glass films as protection and bonding layers in silicon micromachining, Sensors and Actuators, A 41-42, 1994, 338-343

/4/ Woo-Beom Choi et al., Anodic bonding technique under low temperature and low voltage using evaporated glass, J.Vac.Sci.Technol. B 15(2), Mar/Apr 1997, 477-481

/5/ S. Weichel et al., Silicon to silicon wafer bonding using evaporated glass, Sens. Actuators, A 70, 1998, 179-184

/6/ P. Krause et al., Silicon to silicon anodic bonding using evaporated glass, The 8th International Conference on Solid-State Sensors and Actuators, Eurosensors IX. Digest of Technical Papers, Found. Sensors and Actuators Technol., Stockholm, Sweden, June 25-29, 1995, 228-231

/7/ H.J.Quenzer et al., Silicon-silicon anodic bonding with intermediate glass layers using spin-on glasses, Proceedings IEEE, the 9th Annual International Workshop on Micro Electro Mechanical Systems. An Investigation of Micro Structures, Sensors, Actuators, Machines and Systems, 1996, 272-276

/8/ J.J.Gilman, Direct Measurements of the Surface Energies of Crystals, J.Appl.Phys. 31, No.12, 1960, 2208-2218

/9/ P.P.Gillis, J.J.Gilman, Double-Cantilever Cleavage Mode of Crack Propagation, J.Appl.Phys. 35, No.3, 1964, 647-658

/10/ W.P.Maszara et al., Bonding of silicon wafers for silicon-on-insulator, J.Appl.Phys. 64, No.10, 1988, 4943-4950

/11/ W.P.Maszara et al., Role of surface morphology in wafer bonding, J.Appl.Phys. 69, No.1, 1991, 257-260

/12/ A.Plobl, G. Krauter, Wafer direct bonding: tailoring adhesion between brittle materials, Materials Science and Engineering, R25, Nos.1-2, 1999

/13/ U.Aljancic et al., Design and Fabrication of Silicon Piezoresistive Pressure Sensor, XXVI MIPRO 2003, 26th International Convention, May 19-23, 2003, Opatija, Croatia, 46-50

/14/ D.Resnik et al., Direct Bonding of (111) and (100) Oriented Silicon Wafers, Informacije MIDEM 30, 2000, 20-31

/15/ S.T.Lucic et al., Bond-quality characterization of silicon-glass anodic bonding, Sensors and Actuators, A60, 1997, 223-227

/16/ J.A.Plaza et al., Non-destructive in situ test for anodic bonding, Sensors and Actuators, A60, 1997, 176-180

/17/ J.A.Plaza et al., Effect of silicon oxide, silicon nitride and polysilicon layers on the electrostatic pressure during anodic bonding, Sensors and Actuators, A67, 1998, 181-184

/18/ O.Francais et al., Normalized abacus for the global behaviour of diaphragm: pneumatic, electrostatic, piezoelectric or electromagnetic actuation, Journal of Modeling and Simulation of Microsystems, Vol.1, No.2, 1999, 149-160

/19/ U.Aljancic et al., Temperature Behaviour of Diffused Resistors on Thin Silicon Diaphragm, XXVII MIPRO 2004, 27th International Convention, May, 2004, Opatija, Croatia

/20/ U.Aljancic, Simulacija odziva in optimizacija tehnologije silicijevega pizorezistivnega senzorja tlaka, Magistrsko delo, 1993

/21/ T.Rogers et al., Selection of glass, anodic bonding conditions and material compatibility for silicon-glass capacitive sensors, Sensors and Actuators, A46-47, 1995, 113-120

/22/ D.Sparks et al., Reliable Vacuum Packaging Using NanoGetters^{TM} and Glass Frit Bonding, Invited Paper, Reliability, Testing and Characterization of MEMS/MOEMS III, Proc. SPIE Vol.5343, Jan 2004, 70-78

Uroš Aljančič, D. Resnik, D. Vrtačnik, M. Možek, S. Amon
University of Ljubljana, Faculty of Electrical Engineering
Laboratory of Microsensor Structures and Electronics - LMSE
Trzaska 25, 1000 Ljubljana, Slovenia
E-mail: Uros.Aljancic@fe.uni-lj.si

Prispelo (Arrived): 10.09.2004 Sprejeto (Accepted): 15.09.2004